Original Article

6,6′-Bieckol induces apoptosis and suppresses TGF-β-induced epithelial-mesenchymal transition in non-small lung cancer cells

Yongxin Li, Man Liu, Kunlong Yang, Jun Tian *

Department of Biomedicine and Food Science, School of Life Science, Jiangsu Normal University, Xuzhou 221116, China

A R T I C L E   I N F O

A B S T R A C T

Objective: In this study, the aim was to investigate the inhibitory effect of 6,6′-bieckol on the migration and epithelial-mesenchymal transition (EMT) of non-small cell lung cancer (NSCLC) cells, and explore its potential molecular mechanisms.
Methods: Cell migration was measured using a CCK8, wound healing, and transwell migration assay. Apoptosis was determined using an Annexin V/propidium iodide staining. Western blotting and immunofluorescence were used to examine the expression level of apoptosis-related proteins and EMT marker proteins.
Results: The results showed that 6,6′-bieckol inhibited migration and induced apoptosis of NSCLC cells. Furthermore, 6,6′-bieckol had significantly up-regulated the E-cadherin and down-regulated Snail1 and Twist1 transcriptional levels. 6,6′-Bieckol might inhibit TGF-β-induced EMT by down-regulating Snail1 and Twist1 and up-regulating E-cadherin in lung cancer cells.
Conclusion: It is suggested that 6,6′-bieckol has the potential to be developed as a therapeutic candidate for lung cancer.

1. Introduction

Non-small cell lung cancer (NSCLC) is a lung cancer disease and has become the first cause of death of malignant tumors in the urban population (Siegel, Miller, & Jemal, 2020). More than 90% of lung cancer patients present with advanced-stage disease, with extensive invasion and metastases, at diagnosis (Chen et al., 2014). Most of the present lung cancer chemo-preventive and chemotherapeutic agents lead to undesirable side effects (Surien, Ghazali, & Masre, 2019). Therefore, it is imperative to discover new agents derived from natural products with fewer side effects and elucidate their potential mechanisms.

Apoptosis is a process of programmed cell death that occurs in multicellular organisms (Dunnick, Brix, Sanders, & Travlos, 2014). The death proteases (Caspases) and the Bcl-2 family of proteins play a key role in programmed cell death. The initiator Caspases-2, -8, -9, and -10 and the effector Caspases-3, -6, and -7 can be activated to mediate apoptosis in response to diverse pro-apoptotic stimuli from outside and inside of the cells (Mohamed et al., 2014). In addition, during cancer progression, cancer cells rely on pro- and anti-apoptotic Bcl-2 family proteins and tend to be addicted to these survival mechanisms (Spets et al., 2002). Apoptosis and epithelial-mesenchymal transition (EMT) are very basic physiological processes. They are independent and interrelated events in normal development and homeostasis (Song, 2007). EMT is a multistep process in which cells acquire molecular alterations such as loss of cell–cell junctions and restructuring of the cytoskeleton (Kalluri & Weinberg, 2009). EMT plays an important role in the metastasis of various malignant tumors. The activation of certain transcription factors induces EMT, which led many researchers to use EMT to investigate anticancer therapy (Elena, Prieto-García, Díaz-García, García-Ruiz, & Agulló-Ortuño, 2017). Various EMT signaling pathways and EMT-related genes have been identified, and recent research has shown that the metastasis of cancer cells can be suppressed by inhibiting EMT (Kay, Yeung, Jing, & Yang, 2017). Numerous signaling pathways that are involved in the regulation of EMT, such as E-cadherin, Snail/Slug, Twist, and TGF-β signaling pathways, are highly activated in metastatic lung cancers (Li, Liu, Xue, Li, & Wen, 2019; Wang et al., 2017).

Traditional Chinese medicine (TCM) is a rich source for the development of new drugs (Ma & Li, 2020). Previous studies showed that 6,6′-bieckol of the phlorotannin compound was isolated from traditional Chinese medicine, *Ecklonia cava* (Li, Wijesekara, Li, & Kim, 2011; Li, Li, Je, & Kim, 2015). Various biological and pharmaceutical activities of 6,6′-bieckol have been

reported, such as anti-oxidation, anti-inflammation, anti-HIV-1 activity, and anti-tumor (Artan et al., 2008; Kim et al., 2016; Park et al., 2014). However, mechanisms underlying the anti-tumor activities of 6,6′-bieckol, and whether or not it can suppress the migration of lung cancer remain largely unknown. In the present study, we evaluated the effect of 6,6′-bieckol on the migration and EMT of NSCLC cells and its mechanism. 6,6′-Bieckol inhibits A549 and H1299 cell migration and TGF-β induced EMT in *vitro* by down-regulating Snail1 and Twist1 and up-regulating E-cadherin in NSCLC cells.

2. Material and methods

2.1. Materials and chemicals

In our previous study, we purified phlorotannin compounds (**1**–**7**) from *E. cava* (Fig. 1A). The dried powder of *E. cava* (10 kg) was extracted by stirring an extraction unit with MeOH for 10 d. The extract was suspended in water and partitioned with *n*-hexane, CH$_2$Cl$_2$, EtOAc, *n*-BuOH in sequence. The EtOAc fraction was subjected to a silica gel flash chromatography eluting with hexane/ EtOAc/MeOH to yield ten subfractions. Subfraction 5 and 6 were purified by Sephadex LH-20 with MeOH only to afford the phlorotannins, including phloroglucinol (**1**), eckol (**2**), fucodiphlor-oethol G (**3**), phlorofucofuroeckol A (**4**), 7-phloroeckol (**5**), dieckol (**6**), and 6,6′-bieckol (**7**) as illustrated in Fig. 1B. The compounds were dissolved in dimethyl sulfoxide (DMSO, Sigma-Aldrich, St. Louis, MO, USA) and employed in experiments in which the final concentration of DMSO in culture medium was adjusted to <0.01%. Primary antibodies used for Western blot and immunofluorescence analysis were purchased from Cell Signaling Technology (Bedford, Massachusetts, USA). Secondary antibodies used for Western blotting were: 800CW goat anti-mouse and 800CW goat anti-rabbit, purchased from LI-COR Biosciences (Nebraska, USA).

2.2. Cell culture

The NSCLC cell lines (A549 and H1299) purchased from American Type Culture Collection (ATCC), were all maintained in complete Dulbecco's Modified Eagle' Medium (DMEM) (Gibco), supplemented with 10% FBS (Gibco), 100 U/mL penicillin and 100 μg/mL streptomycin, at 37 °C in a humidified incubator with 5% CO$_2$.

2.3. CCK8 assay

The cell proliferation was determined using the CCK8 kit and carried out according to our previous protocols. In short, the cells were plated at a density of 1×10^4 cells/well in 96-well multi-plates. After incubation for 24 h, cells were washed with fresh medium and treated with different concentrations (20 μmol/L, 40 μmol/L, 80 μmol/L, and 160 μmol/L) of 6,6′-bieckol. After 24 h or 48 h, 10 μL of CCK-8 solution was added to each well and further incubated for 2 h. Then the absorbance values were detected at a wavelength of 450 nm using a Bio-Rad microplate reader (California, USA). The cell viability was calculated by the optical density (OD) values of treated groups/OD values of control groups × 100%.

2.4. Cell migration assay

The migration assay was performed using a 24-well transwell chamber with polyvinylpyrrolidone-free polycarbonate membranes (8 μm pore size) as previously reported (Li, Himaya, Dewapriya, Zhang, & Kim, 2013). A total of 200 μL cells (2.5×10^5/mL in serum-free medium) were placed in the upper compartment of the migration chamber and placed in 750 μL culture medium (with 10% FBS) in the lower chamber. The transwell was placed into the lower chamber to incubate at 37 °C in 5% CO$_2$ for 12 h. Then it was incubated in a FBS-free medium containing 0.2% BSA in the presence or absence of concentrations (80 μmol/L) of 6,6′-bieckol, dissolved in 10% DMSO for 24 h at 37 °C. In 5% CO$_2$, the invasive cells attached to the lower surface of the inserted membrane and were fixed with 4% formaldehyde, methanol, and stained with 0.5% crystal violet for 10 min. After incubation, the filter inserts were removed from the wells, and the cells on the upper side of the filter were removed using cotton swabs. Finally, the migrating and invading cells were observed with an optical microscope (Leica Microsystems Wetzlar GmbH, Wetzlar, Germany) at 100 × magnification.

2.5. Cell apoptosis detection by flow cytometry

A549 and H1299 cells were seeded at a density of 1×10^6/well in 6-well plates. After the culture for 24 h, 6,6′-bieckol was added to the culture plates, in which the final concentrations of 6,6′-bieckol were adjusted 80 μmol/L in turn, and then the cells were cultured under routine conditions. Twenty-four hours later, the cells were collected and washed with PBS. According to Annexin V-FITC/PI double staining flow cytometry method, Annexin V/FITC and PI were added to the cells, respectively, the cells were dyed for 15 min, and then the cell apoptosis was detected by flow cytometry (BD Biosciences, San Jose, CA, USA).

2.6. Docking calculations

Docking calculations were carried out using Swissdock. (Zoete, Cuendet, Grosdidier, & Michielin, 2011) It is a fully automated protein-small molecule docking web service, accessible via the Swissdock web server (http://www.swissdock.ch/). The structure of the E-cadherin (PDB-1Q1P) protein model was downloaded from RCSB Protein DataBank (PDB). 6,6′-Bieckol and E-cadherin surface binding analysis was performed by molecular graphics program UCSF Chimera 1.12rc.

2.7. Western blot

Western blotting (WB) was performed according to standard procedures. A total of 80 μg protein was separated and transferred onto nitrocellulose membranes. Membranes were then blocked and incubated with primary antibodies at 4 °C overnight. The membranes were then washed and probed with appropriate secondary antibodies. After the final wash, the membranes were visualized using the Odyssey LI-CDR system. All the gray-scale values in the study were obtained using WCIF ImageJ software.

2.8. Immunofluorescence

A549 and H1299 cells were grown in 4-chamber slides in serum-free media and treated with TGF-β (10 ng/mL) or co-treatment with TGF-β (10 ng/mL) and 6,6′-bieckol (80 μmol/L). After 24 h incubation, cells were fixed with 4% paraformaldehyde at 4 °C. Cells were washed with PBS containing 0.1% BSA and incubated with the anti-E-cadherin antibody for 1 h followed by 1 h incubation with fluorescence-tagged secondary antibody, then counterstained with DAPI for 5 min. Finally, the slides were sealed and pictured under the inverted confocal fluorescence microscope (LSCM; Zeiss, Oberkochen, Germany).
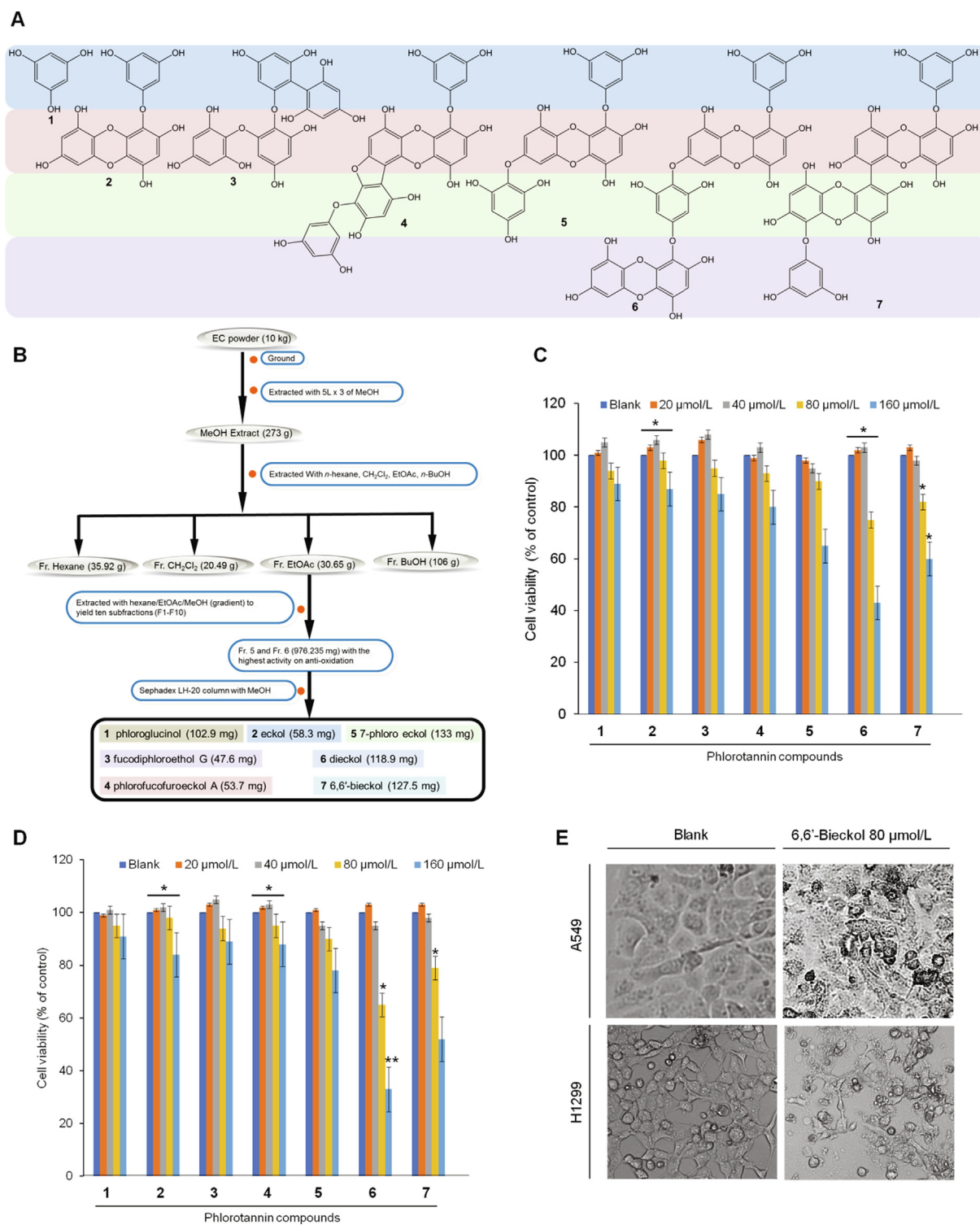
Fig. 1. Chemical structures of phlorotannins compounds (**1–7**) isolated from *E. cava* (A). Extraction, isolation, and purification procedures of phlorotannins (**1–7**) from *E. cava* (B). Cell survival analysis of A549 (C) and H1299 (D) cells treated with different concentrations (20 μmol/L, 40 μmol/L, 80 μmol/L, and 160 μmol/L) of compounds **1–7** at 24 h using CCK8 assays. (E) Morphological changes in A549 and H1299 cells treated with 6,6′-bieckol at 24 h. Images were captured by a phase-contrast microscope. Magnification, ×200. Values are expressed as the mean ± SD of three replicate experiments. *$P < 0.05$; **$P < 0.01$, as compared with blank groups.

2.9. Statistical analysis

The data were shown as the mean of three replicate determinations and standard deviation (SD), statistical comparisons were made with the student's T-test. The values were considered to be significant when *$P < 0.05$ and **$P < 0.01$.

3. Results

3.1. Effect of phlorotannins on cell viability of A549 and H1299 cells

Cytotoxic effects of phlorotannins were tested on cultured A549 and H1299 NSCLC cell lines. Comparisons of the cell growth for

24 h with different concentrations of phlorotannin compounds (**1**–**7**) (20 µmol/L, 40 µmol/L, 80 µmol/L and 160 µmol/L) were shown in Fig. 1C and 1D. In a comparative analysis, 6,6′-bieckol (**7**) showed significant high growth inhibitory effects on the A549 and H1299 cell lines in a dose-dependent manner ($^*P < 0.05$,

$^{**}P < 0.01$). 6,6′-Bieckol inhibited the proliferation of A549 and H1299 cells with the viability percentages of 75%, and 72% (80 µmol/L) at 24 h, respectively, compared to the vehicle-treated blank. Our results showed that 6,6′-bieckol (80 µmol/L for 24 h) had significant anti-proliferative effects on A549 and
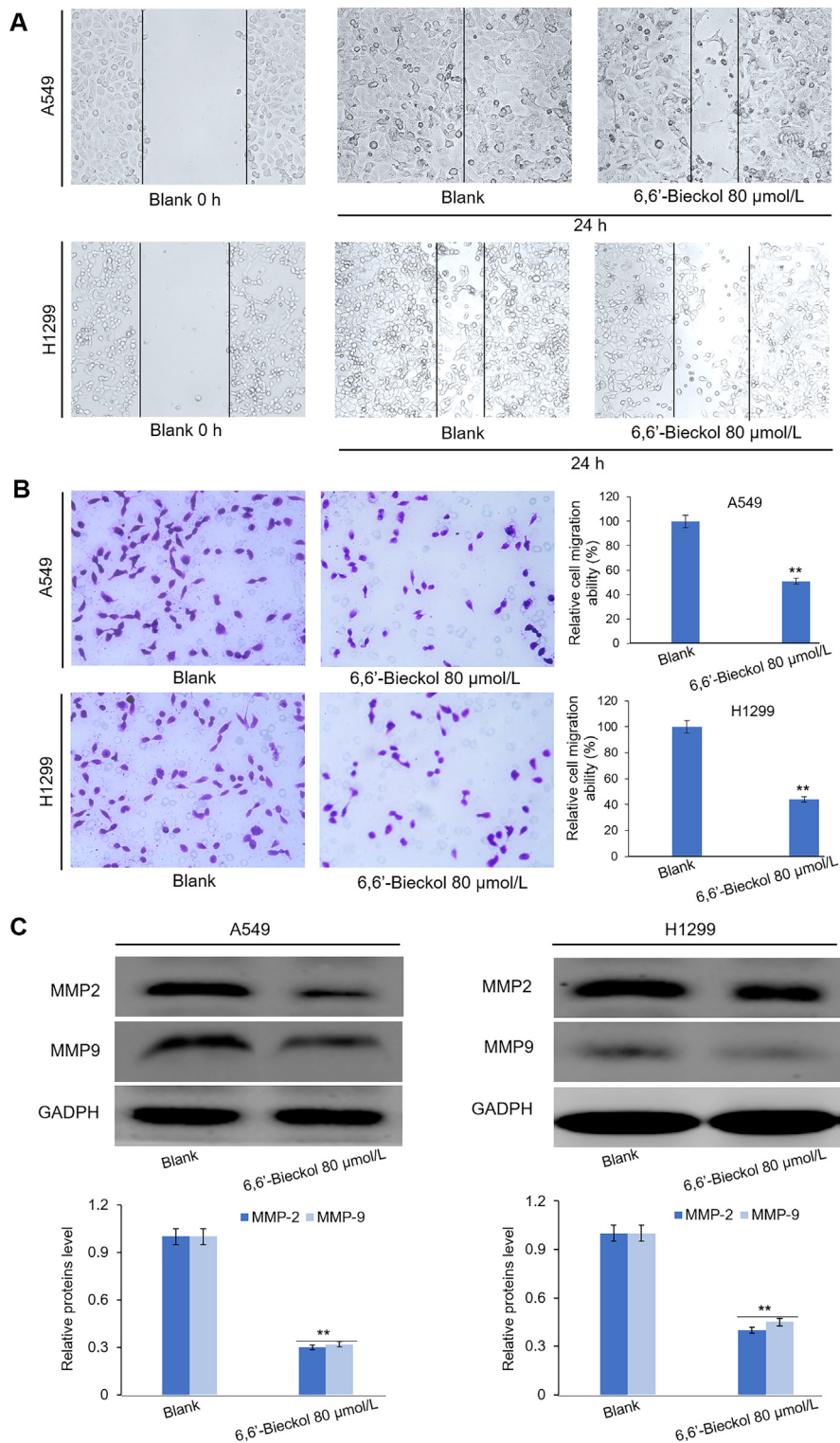

Fig. 2. 6,6′-Bieckol inhibits A549 and H1299 cell migration determined by using wound healing (A) and trans-well assay (B). The results were observed with a microscope at 200× and the relatively blocked percentage (%) of migrated and invaded cells per field were assessed. (C) Protein expression levels of MMP-2 and MMP-9 in treated A549 and H1299 cells. Cell lysates were collected and subjected to SDS-PAGE WB analysis using antibodies specific for MMP-2 and MMP-9. GADPH was used as an internal control. Each value was expressed as the mean ± SD of triplicate experiments. $^*P < 0.05$; $^{**}P < 0.01$, as compared with blank groups.
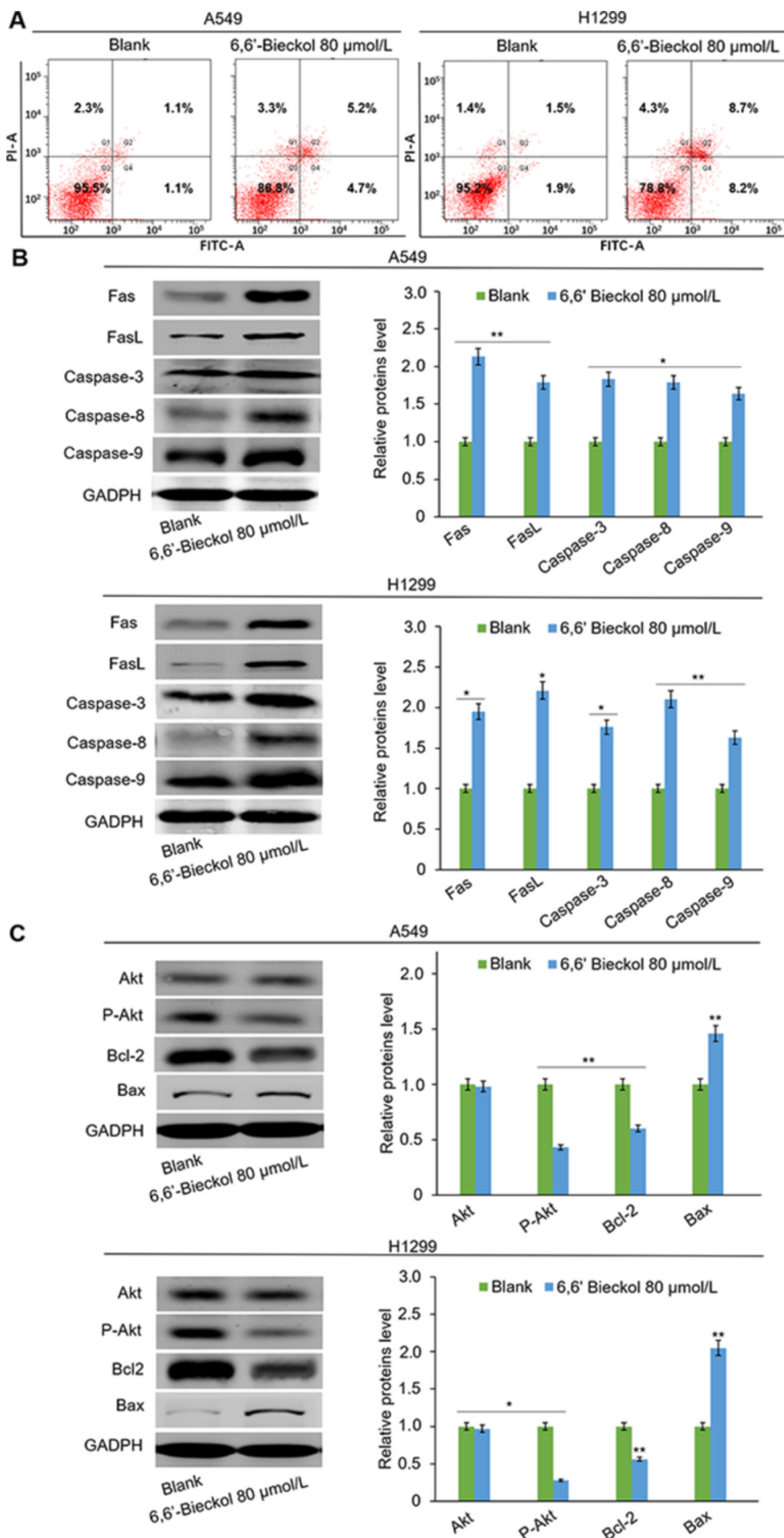
Fig. 3. 6,6′-Bieckol induces apoptosis in A549 and H1299 cells. (A) Cell cycle analysis of A549 and H1299 cells treated with 6,6′-bieckol (80 μmol/L) for 24 h by flow cytometry. (B and C) Expression of apoptosis-related proteins in A549 and H1299 cells treated with 6,6′-bieckol (80 μmol/L) for 24 h. Fas, FasL, and Caspase-8 constitutively activated by 6,6′-bieckol in Western blot detection. (E) Akt phosphorylation was gradually inhibited and Bax/Bcl-2 ratio was increased significantly. Values are expressed as the mean ± SD of three replicate experiments, $^*P < 0.05$; $^{**}P < 0.01$, as compared with blank groups.

H1299 cell lines. After treatment of A549 and H1299 cells with 80 μmol/L 6,6′-bieckol, it was found that the number of cells decreased and condensed compare with the blank group, and a large number of cells separated from the bottom of the culture dish. These changes are very similar to the characteristics of apoptosis and death, indicating that 6,6′-bieckol may have the role of inducing apoptosis as shown in Fig. 1E.

3.2. Effects of 6,6′-bieckol on migration of A549 and H1299 cells

To examine the effect of 6,6′-bieckol on the migration of the cells, a wound-healing assay and transwell migration assay were performed. A549 and H1299 cells were treated with 6,6′-bieckol (80 μmol/L) for 24 h. It was observed that 6,6′-bieckol treatment reduced the A549 and H1299 cell migration in Fig. 2A and B. In these two experiments, 6,6′-bieckol reduced the migration of both cell lines of A549 and H1299 at 80 μmol/L for 24 h compared with the blank. 6,6′-Bieckol blocked the migration of A549 and H1299 with the blocking percentages of 51% and 44% (80 μmol/L) at 24 h, respectively. Western blot results revealed that 6,6′-bieckol treatment of the A549 and H1299 cells resulted in an inhibition of protein expression of both MMP-2 and MMP-9. At the highest concentration (80 μmol/L) of 6,6′-bieckol, there was a significant inhibition in both MMP-2 and MMP-9 and the inhibitory activity was significant ($P < 0.01$) from the concentrations of 0 to 80 μmol/L (Fig. 2C). We found that 80 μmol/L 6,6′-bieckol could effectively inhibit the expression of MMP-2 and MMP-9 in NSCLC cells. The expression of MMP-2 and MMP-9 in A549 and H1299 cells decreased by more than 50%. Therefore, 6,6′-bieckol could inhibit the proliferation of NSCLC cells.

3.3. Induction of apoptosis in A549 and H1299 cells by 6,6′-bieckol

To find out whether apoptosis is induced as an underlying mechanism of anti-proliferation of 6,6′-bieckol treatment, an assessment of apoptosis was performed using a flow cytometer following the staining with Annexin-V/PI. The apoptosis of A549 and H1299 cells treated with 6,6′-bieckol for 24 h were analyzed. As shown in Fig. 3A, the treatment with 80 μmol/L 6,6′-bieckol increased the cell population that was positive for Annexin V and PI staining. Meanwhile, Western blot analysis was carried out to investigate the activation of Fas/FasL and Caspases cascade. As shown in Fig. 3B and C, 6,6′-bieckol not only significantly up-

regulated the expression of Fas/FasL, but also increased downstream proteins Caspase-3, -8, and -9 in a dose-dependent manner. To confirm the expression levels of proteins related to the induction of apoptosis, Bcl-2 (pro-apoptotic product) and Bax (anti-apoptotic product) were analyzed. The results showed that 6,6′-bieckol gradually inhibited Akt phosphorylation and increased Bax/Bcl-2 ratio. As per the results, 6,6′-bieckol exhibited induction of apoptosis in both A549 and H1299 cells. 6,6′-Bieckol down-regulated the anti-apoptotic Bcl-2 levels and as well as up-regulated the pro-apoptotic Bax at protein levels (Fig. 3D and E). These data support the observation of previous experiments that 6,6′-bieckol are inhibiting migration at least in part through the pathway of apoptosis.

3.4. Analysis of binding mode of 6,6′-bieckol to E-cadherin by small-molecule docking

To determine the correlation between 6,6′-bieckol with EMT, a small molecular docking mold to was used to evaluate the binding of 6,6′-bieckol to E-cadherin and their binding sites, as shown in Fig. 4. The best binding model (6,6′-bieckol to 1q1P-E-cadherin) was shown in Fig. 4A. In addition, the three hydroxyl groups of 6,6′-bieckol were predicted to form a hydrogen bond with the polar atoms of residues SER8, LEU21, and PRO5 (Fig. 4B). The experimental results suggested that the 6,6′-bieckol can bind to the pocket of 1q1P-E-cadherin and interact with the key active-site residues, which can result in inhibiting EMT activity.

3.5. Effect of 6,6′-bieckol on TGF-β-induced EMT of A549 and H1299 cells

To investigate the effects of 6,6′-bieckol on protein expressions of EMT markers, a Western blot assay was performed for the proteins extracted from A549 and H1299 cells treated with 6,6′-bieckol (80 μmol/L) for 24 h. The expression of the E-cadherin, Snail1, and Twist1 proteins were investigated to determine whether the effect of 6,6′-bieckol was associated with the inhibition of the TGF-β/Snail1/Twist1 axis by Western blotting. The results showed that TGF-β as an EMT inducer can significantly regulate the expression of EMT-related proteins, such as E-cadherin, Snail1 and Twist1 (Fig. 5A and B). The expression of EMT markers, E-cadherin was significantly increased and Snail1 and Twist1 were significantly decreased by treatment with 6,6′-bieckol (80 μmol/L)
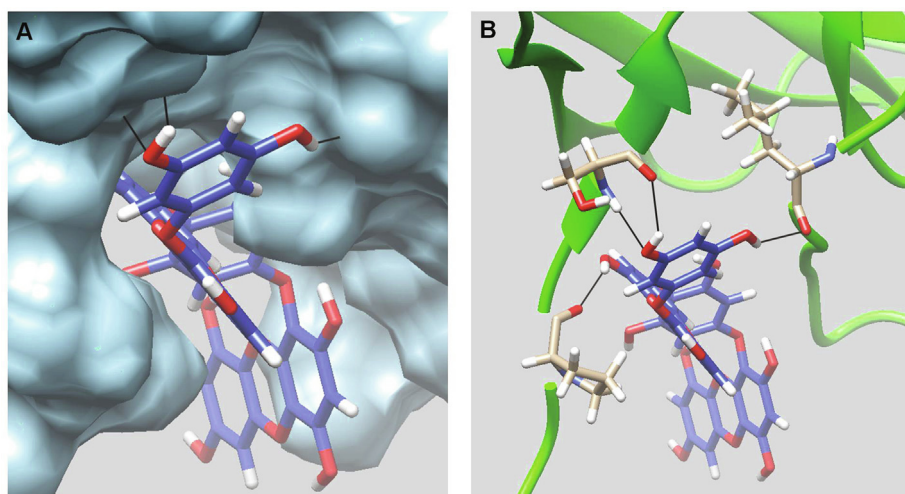

Fig. 4. Molecule binding of 6,6′-bieckol to active site of E-cadherin. (A) Binding mode between 6,6′-bieckol and 1q1p-E-cadherin. Interacting side chains of 1q1p-E-cadherin displayed in surface mode. 6,6′-Bieckol is represented using balls and sticks. (B) The interaction with SER8, LEU21, and PRO5 with the active site has been shown in the figure.
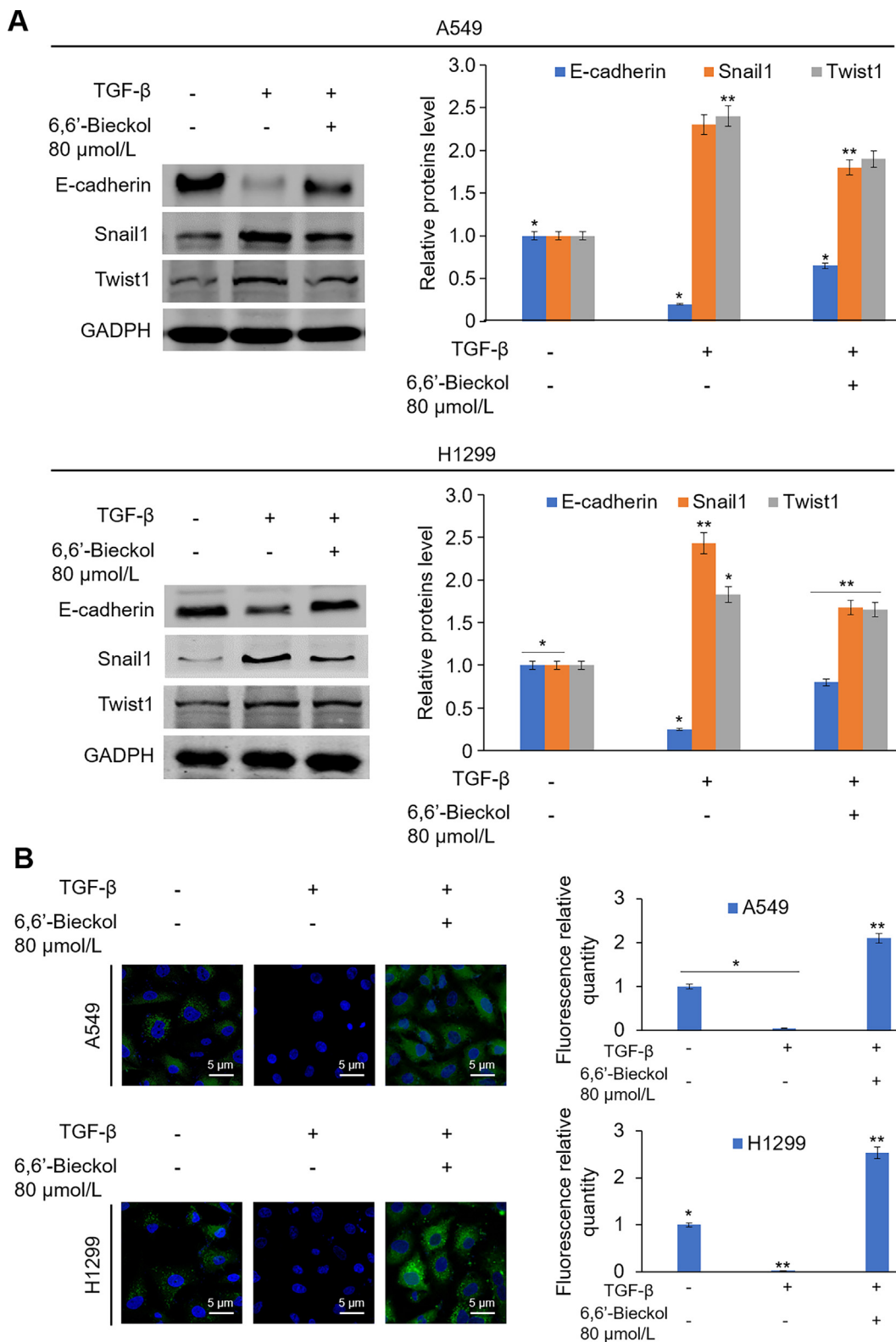
Fig. 5. 6,6′-Bieckol regulates expression level of EMT-associated proteins and inhibits the activation of TGF-β-Snail1/Twist1 signaling. (A) Expression of E-cadherin, Snail1, and Twist1 proteins in A549 and H1299 cells was determined by Western blot. (B) A549 and H1299 Cells were immune-stained with anti-E-cadherin antibody (green color) and nuclei were counterstained with DAPI (blue color) following 6,6′-bieckol treatment. Values are expressed as the mean ± SD of three replicate experiments,*P < 0.05, **P < 0.01 as compared with control groups. Scale bar, 5 μm.

for 24 h compared to that without treatment (Fig. 5A and B). These findings indicated that 6,6′-bieckol could inhibit TGF-β-induced EMT in both A549 and H1299 cells by down-regulating the protein

expression of E-cadherin and up-regulating the protein expression of Snail1, and Twist1. Meanwhile, E-cadherin expression in A549 and H1299 cells was also assessed by immunofluorescence. Consis-

tent with the results of Western blotting, E-cadherin was almost undetectable in TGF-β treated cells; Whereas its expression was significantly recovered by co-treatment with 6,6′-bieckol (80 μmol/L) for 24 h in both A549 and H1299 cells (Fig. 5C). The Western blotting and immunofluorescence results suggested that 6,6′-bieckol had an inhibitory effect on EMT.

4. Discussion

6,6′-Bieckol is a phlorotannin compound isolated from *E. cava*. It exerts immune protective effects in severe inflammatory diseases (Kim et al., 2016). 6,6′-Bieckol has shown remarkable anti-proliferative and inhibited matrix metalloproteinase effects against various types of solid tumors. Furthermore, it has been reported that 6,6′-bieckol significantly inhibits adipocyte differentiation by downregulating adipogenesis and lipogenesis in preadipocytes of a mouse cell line (Kwon et al., 2014). It also inhibits human immunodeficiency virus type-1 induced syncytia formation. (Artan et al., 2008; Karadeniz, Kang, Park, Park, & Kim, 2014). However, the effect of 6,6′-bieckol on the migration of lung cancer cells remains unclear. We investigated these mechanisms of 6,6′-bieckol on NSCLC cells, and 6,6′-bieckol can inhibit lung cancer A549 and H1299 cells migration and TGF-β induced EMT by down-regulating TGF/β-Snail1/Twist1 signaling pathway.

EMT is an important developmental process that is also implicated in disease pathophysiologies, such as the migration, invasion, and metastasis of cancer (Li and Li, 2015; Mittal, 2018). TGF-β induces EMT in various cancer cells, increasing their invasion and migration and resulting in enhancing metastasis (Huang et al., 2016; Nirajan et al., 2016). EMT depends on a reduction in expression of cell adhesion molecules and loss of tight junctions. The previous studies have shown that regulation of EMT may represent an emerging therapeutic approach against NSCLC (Chae et al., 2016). In our present study, it was found that 6,6′-bieckol could inhibit TGF-β induced EMT, increasing E-cadherin expression and reducing the invasiveness and migration in the NSCLC A549 and H1299. We also found that Snail1/Twist1 signaling is required for TGF-β-induced EMT in NSCLC cells, which clarifies the mechanism by which 6,6′-bieckol may inhibit NSCLC cell metastasis.

Apoptosis is the key characteristic of anticancer drugs as it plays an important role in the development, the regulation of hematopoietic progenitor cells. The sustained genetic damage or that undergo uncontrolled cellular proliferation in the elimination of cells (Bosserman et al., 2015; Fulda & Debatin, 2006). It is also a complex process controlled by many factors, such as Bcl-2 family proteins and Caspases (Kale, Osterlund, & Andrews, 2017). The Bcl-2 protein, located in the mitochondrial membrane, is an effective inhibitor of apoptosis. It plays an important role in promoting cell survival and inhibiting the actions of pro-apoptotic proteins (García-Sáez, 2012). The Caspases play a role in programmed cell death (Shalini, Dorstyn, Dawar, & Kumar, 2015). The present study demonstrated that 6,6′-bieckol exhibited anti-proliferative effect and apoptosis against A549 and H1299 cells. In this study, we found that 80 μmol/L 6,6′-bieckol could induce apoptosis against A549 and H1299 cells. These results suggested that 6,6′-bieckol induced apoptosis through Bcl-2 and Caspases proteins in the NSCLC cells.

5. Conclusion

In conclusion, the compound of 6,6′-bieckol isolated from *E. cava* showed significant inhibitive effects on cell proliferation in A549 and H1299 cells. 6,6′-Bieckol also exhibited cytotoxicity by inducing apoptosis in A549 and H1299 cells via modulation of Bcl-2, Bax, Caspase-3, -8, and -9. Additionally, our results confirmed that 6,6′-bieckol can inhibit the migration, block the EMT process of A549 and H1299 cells, and these effects may be associated with its inhibition on the activation of the TGF/β-Snail1/Twist1 signaling pathway (Fig. 6). Therefore, our results suggest that 6,6′-bieckol has a potential to be developed as a therapeutic candidate for lung cancer.
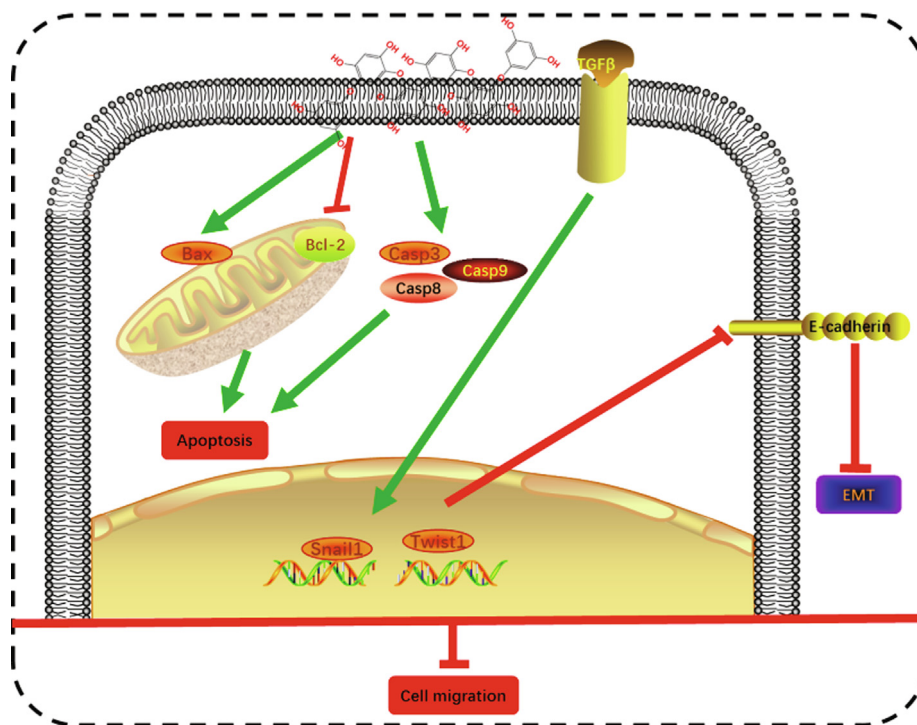

Fig. 6. 6,6′-Bieckol inhibits cell migration in NSCLC cells by inducing apoptosis and inhibiting TGF-β induced EMT.

Declaration of Competing Interest

The authors declare that they have no known competing financial interests or personal relationships that could have appeared to influence the work reported in this paper.

Acknowledgments

References

Artan, M., Li, Y., Karadeniz, F., Lee, S. H., Kim, M. M., & Kim, S. K. (2008). Anti-HIV-1 activity of phloroglucinol derivative, 6,6′-bieckol, from ecklonia cava. *Bioorganic & Medicinal Chemistry, 16*(17), 7921–7926.

Bosserman, L., Rogers, K., Willis, C., Davidson, D., Whitworth, P., Karimi, M., Upadhyaya, G., Rutledge, J., Hallquist, A., Perree, M., & Presant, C. A. (2015). Application of a drug-induced apoptosis assay to identify treatment strategies in recurrent or metastatic breast cancer. *PloS One, 10*(5), e0122609.

Chae, Y. K., Chang, S., Ko, T., Anker, J., Agte, S., Iams, W., Choi, W. M., Lee, K., & Cruz, M. (2016). Epithelial-mesenchymal transition (EMT) signature is inversely associated with T-cell infiltration in non-small cell lung cancer (NSCLC). *Scientific Reports, 8*(1). https://doi.org/10.1038/s41598-018-21061-1.

Dunnick, J. K., Brix, A., Sanders, J. M., & Travlos, G. S. (2014). Apoptosis: A review of programmed cell death. *Toxicologic Pathology, 35*(4), 495–516.

Elena Prieto-García Díaz-García, C. V., García-Ruiz, I., & Agulló-Ortuño, M. T. (2017). Epithelial-to-mesenchymal transition in tumor progression. *Medical Oncology, 34*(7). 122–122.

Fulda, S., & Debatin, K. M. (2006). Extrinsic versus intrinsic apoptosis pathways in anticancer chemotherapy. *Oncogene, 25*(34), 4798–4811.

García-Sáez, A. J. (2012). The secrets of the Bcl-2 family. *Cell Death & Differentiation, 19*(11), 1733–1740.

Huang, S. F., Horng, C. T., Hsieh, Y. S., Hsieh, Y. H., Chu, S. C., & Chen, P. N. (2016). Epicatechin-3-gallate reverses TGF-beta 1-induced epithelial-to-mesenchymal transition and inhibits cell invasion and protease activities in human lung cancer cells. *Food & Chemical Toxicology, 94*(2016), 1–10.

Kale, J., Osterlund, E. J., & Andrews, D. W. (2017). BCL-2 family proteins: Changing partners in the dance towards death. *Cell Death & Differentiation, 25*(1), 65–80.

Kalluri, R., & Weinberg, R. A. (2009). The basics of epithelial-mesenchymal transition. *Journal of Clinical Investigation, 119*(6), 1420–1428.

Karadeniz, F., Kang, K. H., Park, J. W., Park, S. J., & Kim, S. K. (2014). Anti-HIV-1 activity of phlorotannin derivative 8,4-dieckol from Korean brown alga *Ecklonia cava. Bioscience Biotechnology & Biochemistry, 78*(7), 1151–1158.

Kay Yeung Jing & Yang (2017). Epithelial-mesenchymal transition in tumor metastasis. *Molecular Oncology, 11*(1), 28–39.

Kwon, T. H., Wu, Y. X., Kim, J. S., Woo, J. H., Park, K. T., Kwon, O. J., et al. (2014). 6,6′-bieckol inhibits adipocyte differentiation through downregulation of adipogenesis and lipogenesis in 3t3-l1 cells. *Journal of the Science of Food and Agriculture, 95*(9), 1830–1837.

Kim, A. R., Lee, B., Joung, E. J., Gwon, W. G., Utsuki, T., Kim, N. G., et al. (2016). 6,6′-bieckol suppresses inflammatory responses by down-regulating nuclear factor-κb activation via akt, jnk, and p38 mapk in lps-stimulated microglial cells. *Immunopharmacology & Immunotoxicology, 38*(3), 244–252.

Li, L., & Li, W. (2015). Epithelial-mesenchymal transition in human cancer: Comprehensive reprogramming of metabolism, epigenetics, and differentiation. *Pharmacology & Therapeutics, 150*, 33–46.

Li, L., Liu, J., Xue, H., Li, C., & Wen, T. (2019). A TGF-β-MTA1-SOX4-EZH2 signaling axis drives epithelial–mesenchymal transition in tumor metastasis. *Oncogene, 39*(1), 1–15.

Li, Y. X., Himaya, S. W. A., Dewapriya, P., Zhang, C., & Kim, S. K. (2013). Fumigaclavine C from a marine-derived fungus *Aspergillus fumigatus* induces apoptosis in MCF-7 breast cancer cells. *Marine Drugs, 11*(12), 5063–5086.

Li, Y. X., Li, Y., Je, J. Y., & Kim, S. K. (2015). Dieckol as a novel anti-proliferative and anti-angiogenic agent and computational anti-angiogenic activity evaluation. *Environmental Toxicology & Pharmacology, 39*(1), 259–270.

Li, Y. X., Wijesekara, I., Li, Y., & Kim, S. K. (2011). Phlorotannins as bioactive agents from brown algae. *Process Biochemistry, 46*(12), 2219–2224.

Ma, B. N., & Li, X. J. (2020). Resveratrol extracted from Chinese herbal medicines: A novel therapeutic strategy for lung diseases. *Chinese Herbal Medicines, 12*(4), 349–358.

Mittal, V. (2018). Epithelial mesenchymal transition in tumor metastasis. *Annual Review of Pathology: Mechanisms of Disease, 13*(1), 395–412.

Mohamed, H., Hidemichi, W., AliSakuragi, A., ... Sakuragi (2014). Apoptosis and molecular targeting therapy in cancer. *Biomed Research International, 2014*, 1–23.

Nirajan, S., Lokendra, C., Han, M. K., Lee, S. O., Kim, C. Y., & Jeong, Y. (2016). Glutamine inhibits CCl4 induced liver fibrosis in mice and TGF-β1 mediated epithelial-mesenchymal transition in mouse hepatocytes. *Food & Chemical Toxicology, 93*, 129–137.

Park, M. H., Heo, S. J., Park, P. J., Moon, S. H., Sung, S. H., Jeon, B. T., et al. (2014). 6,6′-bieckol isolated fromecklonia cavaprotects oxidative stress through inhibiting expression of ros and proinflammatory enzymes in high-glucose-induced human umbilical vein endothelial cells. *Applied Biochemistry and Biotechnology, 174*(2), 632–643.

Shalini, S., Dorstyn, L., Dawar, S., & Kumar, S. (2015). Old, new and emerging functions of caspases. *Cell Death & Differentiation, 22*(4), 526–539.

Siegel, R. L., Miller, K. D., & Jemal, A. (2020). Cancer statistics, 2020. *CA: A Cancer Journal for Clinicians, 70*(1), 7–30.

Song, J. (2007). EMT or apoptosis: A decision for TGF-β. *Cell Research, 17*(4), 289–290.

Spets, H., Strömberg, T., Georgii-Hemming, P., Siljason, J., Nilsson, K., & Jernberg-Wiklund, H. (2002). Expression of the bcl-2 family of pro- and anti-apoptotic genes in multiple myeloma and normal plasma cells. *European Journal of Haematology, 69*(2), 76–89.

Surien, O., Ghazali, A. R., & Masre, S. F. (2019). Lung cancers and the roles of natural compounds as potential chemotherapeutic and chemopreventive agents. *Biomedical and Pharmacology Journal, 12*(1), 85–98.

Wang, Y., Wang, H., Zhou, R., Zhong, W., Lu, S., Ma, Z., et al. (2017). Baicalin inhibits human osteosarcoma cells invasion, metastasis, and anoikis resistance by suppressing the transforming growth factor-β1-induced epithelial-to-mesenchymal transition. *Anti-cancer Drugs, 28*(6), 581.

Chen, Z., Fillmore, C. M., Hammerman, P. S., Kim, C. F., & Wong, K. K. (2014). Non-small-cell lung cancers: A heterogeneous set of diseases. *Nature Reviews Cancer, 14*(8), 535–546.

Zoete, V., Cuendet, M. A., Grosdidier, A., & Michielin, O. (2011). SwissParam: A fast force field generation tool for small organic molecules. *Journal of Computational Chemistry, 32*(11), 2359–2368.